Technical Physics Letters, 2022, Vol. 48, No. 10

06.5;05.1;15.1

A new method for synchrotron radiation x-ray imaging of micro-objects using nanofocusing optics and tomography

© V.G. Kohn[1], T.S. Argunova[2]

[1] National Research Centre „Kurchatov Institute", Moscow, Russia
[2] Ioffe Institute, St. Petersburg, Russia
E-mail: argunova@mail.ioffe.ru

Received August 3, 2022
Revised August 19, 2022
Accepted August 22, 2022

A new absorption-based method for studying the internal structure of micro-objects using synchrotron radiation is proposed. The method registers the integral intensity of the beam after passing through the object, and the locality is achieved by focusing the beam with a refractive lens into a nanometer-wide line. In this case, phase contrast is not utilized, the result is obtained immediately, and two-dimensional images of an object are calculated by computed tomography. The method does not require complex mathematical calculations and gives high accuracy results. Model experiments using a silicon carbide substrate and some other parameters were performed for illustrative purposes.

Keywords: Synchrotron Radiation, micro-objects, nanofocusing, tomography, micropores.

DOI: 10.21883/TPL.2022.10.54793.19333

The development of industrial growth processes for bulk crystals of silicon carbide (SiC) and sapphire (α-Al_2O_3) led to an enhancement of their structural uniformity. However, substrates made from these crystalline materials, which are used widely in electronics, may contain pores (SiC) or gaseous inclusions (Al_2O_3) with their sizes reduced to submicrometer or nanometer scales. The properties of epitaxial nanoheterostructures or graphene produced by thermal decomposition of SiC [1] or deposition on sapphire [2] depend on the quality of substrates. This imposes strict requirements on diagnostic methods. X-ray techniques play an essential role here by bridging the gap between optical and electron microscopy.

Synchrotron radiation (SR) may be used to study the internal structure of micrometer-sized objects. However, the simple „in-line"experimental design, where the absorption of rays propagating through an object is considered, is not applicable to microobjects, since absorption is combined in this case with phase contrast (i.e., local variation of the radiation intensity due to the phase difference of rays propagating through an object and past it [3]). This variation does not affect the integrated intensity and averages to zero. If an object is large, phase contrast averages out even in coherent radiation, since the oscillation period is fairly small; therefore, high-resolution detectors are not needed.

When the studied object grows smaller, it becomes necessary to use either high image magnification (i.e., X-ray microscopy) or a high-resolution detector. Absorption becomes less significant in this case, while phase contrast has a relatively large period and is well-pronounced. High coherence is not needed to observe phase contrast, but is required to solve the inverse problem properly. The core of the matter is that phase contrast precludes the direct determination of $t(x, y)$ (the thickness of an object under the beam as a function of coordinates in the plane perpendicular to the beam), which is hereinafter referred to as the object image. Methods for calculating $t(x, y)$ from the intensity $I(x, y)$ measured by a coordinate detector are needed. If absorption and phase contrast are both present, the inverse problem is solved inexactly.

Absorption is often neglected in solving it, since the intensity variations due to phase contrast are more significant than the variations due to absorption. However, tight control of the degree of coherence is needed in such experiments. This applies to all methods, including both X-ray microscopy and coherent diffraction imaging and ptychography techniques [4]. It is rather difficult to control the degree of coherence, since it may be affected adversely by various factors (not just the physical size of a source). A high-resolution (normally around $1\,\mu$m) coordinate detector is essential for such studies, but not everyone can afford an instrument of this kind.

We propose a fundamentally different imaging method for microobjects that relies entirely on absorption. It allows one to obtain function $t(x, y)$ without solving the inverse phase contrast problem and at any degree of partial coherence. Phase contrast is obviated via measurements of the integrated radiation intensity performed with the use of a detector summing all transmitted photons behind the sample: it averages out, and the intensity variations are governed solely by absorption.

The locality of information on the object data is achieved by beam nanofocusing with a planar compound refractive lens (CRL) [5]. The CRL manufacturing technology has now become more complex, and the quality of CRLs increased greatly. Specifically, planar nanofocusing CRLs

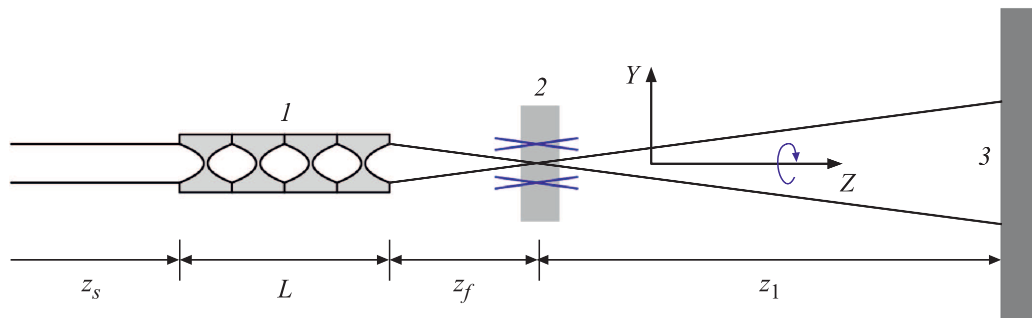

Figure 1. Diagram of the experiment. *1* — Compound refractive lens, *2* — sample, *3* — detector, z_s — source–lens distance, L — lens length, z_f — focal distance, z_1 — sample–detector distance. An SR beam moves vertically along the sample at each angle of rotation of the sample about axis Z.

capable of focusing a beam to a size no greater than 20 nm have become available [6]. Online programs for calculating all the parameters of beams focused by such CRLs have also been developed [7].

The diagram of an experiment for the new method is presented in Fig. 1. An SR beam reflected by a monochromator (not shown) is focused by a planar CRL in the vertical direction, since the vertical size of an SR source is smaller than the horizontal one. A sample (e.g., SiC crystal containing micrometer-sized pores of various shapes) is positioned at focal distance z_f from the CRL. A detector is mounted at arbitrary distance z_1 and measures all radiation reaching it. The planar CRL focuses the beam only along axis Y. Locality along axis X is not available, and the beam is restricted only by the slit.

The planar CRL has the capacity to form a linear harrow beam up to 70 μm in length. The slit may restrict it to smaller values. One point of dependence $I(y)$ integrated along coordinate x is obtained this way. Shifting the CRL along axis Y in small steps, one obtains all the needed points. The step size is chosen so as to provide the needed imaging precision. Piezo movers capable of shifting a sample in very small steps (just several nanometers) are currently available. The method described above allows one to obtain a dependence of intensity integrated along coordinate x on coordinate y. No CRLs capable of focusing a beam to a nanometer-sized circle are available at present, and it is still unclear how this may actually be done.

Tomography may be used to obtain dependence $I(x, y)$. In order to do this, one needs to rotate a sample about axis Z and obtain a sinogram, which is a two-dimensional data set $I(y, \varphi)$ (φ is the rotation angle). This is illustrated schematically in Fig. 1. The mentioned rotation should be performed within the angle interval of 0–180° in steps of a fixed magnitude, and vertical displacement of a focused beam should be carried out at each angular position. Using tomography software, one may then convert the obtained sinogram into a tomogram (i.e., dependence $I(x, y)$). The sought-for $t(x, y)$ dependence is determined by logarithmating and multiplying by a constant factor.

This method obviates the need for ambiguous mathematical calculations. Its resolution is set by the beam size at the lens focus. SR coherence is still needed here, since focusing is a special case of phase contrast, and the beam size at the lens focus is specified both by the CRL and the transverse size of an SR source. However, coherence may be partial. This lowers the resolution, but does not result in any substantial errors.

The method differs from common tomography in that a tomogram needs to be logarithmated instead of a sinogram. We obtain an intensity integrated along transverse coordinate x. Common tomography yields function $t(x, y)$ directly, while we determine function $I(x, y)$. This is what determines the peculiarity of the method. If the FBP (filtered back projection) algorithm is used [8], a Fourier transform over a finite domain is calculated. It is assumed that the function is zero outside of this domain and at its boundaries.

However, function $I(x, y)$ cannot assume a zero value. If we normalize it to unity outside of an object, it will be equal to unity. A jump is then obtained at the domain boundary, and this jump induces a strong artifact. It consists in the fact that the background of an object (i.e., function $t(x, y)$) is near-zero only at the center of the domain and increases greatly as one gets closer to the boundaries. This may be rectified in the following way. When normalizing the intensity outside of an object to unity, one needs to subtract unity at each object point in the calculation of a sinogram (i.e., subtract the number of grid points from each sinogram value) and then add this unity to each tomogram point. The artifact is thus suppressed.

Since contrast in the considered method is set by absorption only, it will be weak for microobjects, and soft radiation with a low photon energy is better suited for experiments. At the same time, a large number of photons are needed so that the obtained contrast would not be impaired by shot noise, the relative value of which is equal to unity divided by the square root of the number of photons. In other words, the samples used in studies of pores in crystals need to be as thin as possible.

To illustrate the capabilities of the method, we performed a computer simulation of an experiment with the following parameters: photon energy — 6.2 keV; vertical source size — 100 μm; CRL–source distance $z_s = 14$ m; a planar CRL on a silicon surface has ten elements with an aperture of 50 μm, a curvature radius of 6.25 μm, and a thickness of 2 μm of the material layer between parabolic surfaces. The online program [7] yields a FWHM of the Gaussian intensity curve at the lens focus of 0.332 μm for the indicated parameters, while the FWHM for a point source is 0.282 μm; i.e., the source size contributes to just a slight increase in the FWHM of a beam at the lens focus. Focal distance $z_f = 2.39$ cm.

The sample is a crystalline SiC wafer with pores of various size and shape. Figure 2, *a* presents function $t(x, y)$ for such objects. Black areas ($t = 0$) are the regions where no objects are present. This is the minimum pore thickness. The maximum is $t_{\max} = 8\,\mu$m (white color). The calculation domain was 25.6 μm in size. A grid with a pitch of 0.1 μm and 256 points was used. The grid pitch corresponds to the vertical scan step of the focused beam through the sample. Figure shows two spheres with diameters of 4 and 8 μm and an ellipsoid with diameters of 2, 12, and 8 μm along axes X, Y, and Z, respectively.

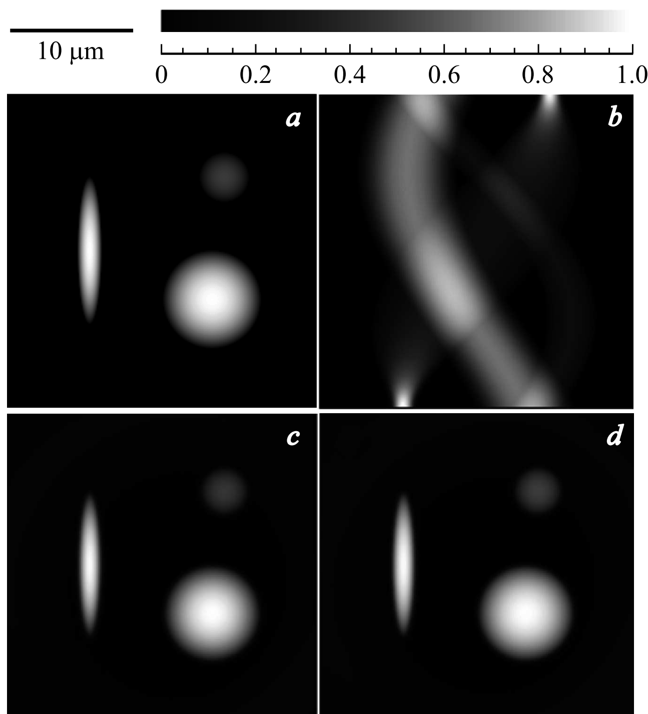

Figure 2. Four different functions in plane (X, Y), which is perpendicular to an SR beam, in a square region with a linear size of 25.6 μm. *a* — Function $t(x, y)$ of the initial sample thickness, *b* — sinogram, *c* — tomogram, and *d* — calculated function $t(x, y)$. All functions are shown in the interval from the minimum to the maximum values, which is normalized to interval (0, 1). The actual minimum and maximum values for each function are given in the text. Axis Y is directed vertically.

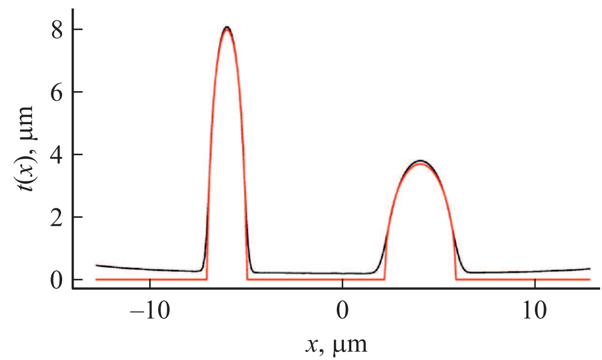

Figure 3. Detailed comparison of the initial (red curve with zero background) and calculated (black curve with above-zero background) functions $t(x, y)$ on axis X at $y = 12.2\,\mu$m.

These data were used to calculate the sinogram shown in Fig. 2, *b*. The horizontal size here is also 25.6 μm, and the vertical size corresponds to an angle interval from −90 to 90°, which was calculated in steps of 1°. Function $t(x, y)$ was used to calculate $I(x, y) = \exp[Mt(x, y)]$, where $M = 0.02998\,\mu\text{m}^{-1}$. A void in a material enhances the intensity, which is normalized to unity where no such void is present. Function $I(x, y)$ was summed over all points along axis X at different values of angle φ of sample rotation about axis Z. This corresponded to sinogram $I(y, \varphi)$. The beam size at the lens focus was taken into account by calculating a convolution of the y-dependence at each angle with a Gaussian function with a FWHM of 0.332 μm (see above). In addition, the number of points (256) was subtracted at each point of the y-dependence to obtain a zero-valued minimum. It turned out that the sinogram minimum is zero to high precision, and the maximum is 24.5 μm.

The sinogram simulates experimental data. A tomogram was calculated using proprietary software. A unit was added to each point after calculation. The obtained result is shown in Fig. 2, *c*. As before, black and white areas correspond to the minimum and maximum contrast, but the minimum is now 1.006, and the maximum is 1.277. The contrast determined as a ratio of the difference of these values to their sum is 0.12, which is not that low. Dependence $t(x, y)$ is obtained by logarithmating the tomogram and dividing by M. The result is presented in Fig. 2, *d*. The visual difference between Figs. 2, *a* and *d* is negligible, but this is attributable to the fact that the resolution is fairly low.

The first difference is in the minimum and maximum values, which are 0.19 and 8.15 nm, respectively, in Fig. 2, *d*. Figure 3 presents the comparison of the initial $t(x)$ curve at height $y = 12.2\,\mu$m and the curve calculated based on the sinogram with the beam size taken into account. It is evident that the method generally characterizes objects well, but cannot reproduce accurately sudden variations in thickness at their boundaries and the actual lack of an object. Although the background is not that high, it is still nonzero. Narrower beams are needed to enhance the accuracy.

Funding

The work of V.G. Kohn was supported by the Ministry of Science and Higher Education of the Russian Federation (project 075-15-2021-1362) and, partially, by the Russian Foundation for Basic Research (grant No. 19-29-12043 mk). The work of T.S. Argunova was supported financially by the Russian Foundation for Basic Research (grant No. 19-29-12041mk) and, partially, by the Ministry of Science and Higher Education of the Russian Federation (project 075-15-2021-1349).

Conflict of interest

The authors declare that they have no conflict of interest.

References

[1] A.A. Lebedev, S.Yu. Davydov, I.A. Eliseyev, A.D. Roenkov, O. Avdeev, S.P. Lebedev, Y. Makarov, M. Puzyk, S. Klotchenko, A.S. Usikov, Materials, **14** (3), 590 (2021). DOI: 10.3390/ma.14030590

[2] J. Shan, J. Sun, Z. Liu, ChemNanoMat, **7** (5), 515 (2021). DOI: 10.1002/cnma.202100079

[3] A. Snigirev, I. Snigireva, V. Kohn, S. Kuznetsov, I. Schelokov, Rev. Sci. Instrum., **66** (12), 5486 (1995). DOI: 10.1063/1.1146073

[4] J.-Y. Buffiere, J. Baruchel, in *Synchrotron radiation: basics, methods and applications*, ed. by S. Mobilio, F. Boscherini, C. Meneghini (Springer-Verlag, Berlin–Heidelberg–N.Y.–Dordrecht–London, 2015), p. 389. DOI: 10.1007/978-3-642-55315-8

[5] A. Snigirev, I. Snigireva, V. Kohn, V. Yunkin, S. Kuznetsov, M.V. Grigoriev, T. Roth, G. Vaughan, C. Detlefs, Phys. Rev. Lett., **103** (6), 064801 (2009). DOI: 10.1103/PhysRevLett.103.064801

[6] V.G. Kohn, M.S. Folomeshkin, J. Synchrotron Rad., **28** (2), 419 (2021). DOI: 10.1107/S1600577520016495

[7] http://kohnvict.ucoz.ru/jsp/1-crlpar.htm

[8] A.C. Kak, M. Slaney, *Principles of computerized tomographic imaging* (IEEE Press, N.Y., 1988).